

# On generating fatigue crack growth thresholds

Scott C. Forth <sup>a,\*</sup>, James C. Newman Jr <sup>b</sup>, Royce G. Forman <sup>c</sup>

<sup>a</sup> NASA Langley Research Center, 2 West Reid Street, Mail Stop 188E, Hampton, VA 23681, USA

<sup>b</sup> Department of Aerospace Engineering, 330 Walker Engineering Lab., Hardy Street, Mississippi State University, Mississippi State, MS 39762, USA

<sup>c</sup> NASA Johnson Space Center, 2101 NASA Road 1, Mail Code EM2, Houston, TX 77058, USA

Received 3 October 2001; received in revised form 18 April 2002; accepted 17 May 2002

## Abstract

The fatigue crack growth threshold, defining crack growth as either very slow or nonexistent, has been traditionally determined with standardized load reduction methodologies. These experimental procedures can induce load history effects that result in crack closure. This history can affect the crack driving force, i.e. during the unloading process the crack will close first at some point along the wake or blunt at the crack tip, reducing the effective load at the crack tip. One way to reduce the effects of load history is to propagate a crack under constant amplitude loading. As a crack propagates under constant amplitude loading, the stress intensity factor range,  $\Delta K$ , will increase, as will the crack growth rate,  $da/dN$ . A fatigue crack growth threshold test procedure is experimentally validated that does not produce load history effects and can be conducted at a specified stress ratio,  $R$ . The authors have chosen to study a ductile aluminum alloy where the plastic deformations generated during testing may be of the magnitude to impact the crack opening.

Published by Elsevier Science Ltd.

**Keywords:** Fatigue; Threshold; Crack growth; Test methods; Crack closure

## 1. Introduction

Fatigue crack growth in a material is typically quantified by the size of the crack,  $a$ , the rate at which it propagates,  $da/dN$ , and the linear-elastic fracture mechanics term,  $\Delta K$ , the stress intensity factor range. The relationship between crack growth rate and stress intensity was originally shown to be linear over two orders of fatigue crack growth rates on a log–log scale [1]. However, this relation is nonlinear near fracture [2], and when the crack growth rate approaches threshold [3].

The fatigue crack growth threshold is the asymptotic value of  $\Delta K$  at which  $da/dN$  approaches zero [4]. It has been shown that cracks propagate at a  $\Delta K$  below the threshold value [5–8] defined using the ASTM standardized (E647) constant  $R$  load reduction test procedure [9]. The constant  $R$  load reduction method reduces the

maximum and minimum load applied to a cracked specimen such that the load ratio,  $R$  ( $R = K_{\min}/K_{\max} = P_{\min}/P_{\max}$ ) remains constant. Experimental results suggest that the constant  $R$  load reduction test procedure can develop crack closure levels above the steady-state magnitude [10,11]. This closure is generated when initiating the test at a high load, and shedding load until threshold is reached. This produces larger plastic strains at the high loads early in the test than in subsequent loads near threshold. This plastic history can affect the crack driving mechanisms at low  $R$  values by prematurely unloading the crack tip due to crack face contact [12,13], i.e. the local opening stress at the crack tip is less than the applied load should impart.

ASTM standard E647 on fatigue crack growth rate determination also defines a constant  $K_{\max}$  test procedure for threshold definition. This method imposes a constant  $K_{\max}$  [14,15] while increasing  $K_{\min}$ . The utilization of this procedure purportedly develops a threshold that is uninfluenced by plasticity-induced crack closure. There exists, however, several stipulations on this procedure that make it undesirable for generating a range of thresh-

\* Corresponding author. Tel.: +1-757-864-3823; fax: +1-757-864-8911.

E-mail address: s.c.forth@larc.nasa.gov (S.C. Forth).

hold values. First, the threshold determined cannot be generated reliably at a specific  $R$  value [16]. Second, the methodology is still reliant on load reduction procedures to determine threshold, which can introduce load history effects [17]. Finally, there has been evidence that the value chosen for  $K_{\max}$  can have a significant impact on the threshold generated and in some cases introduces creep effects [18–20].

The fatigue crack growth thresholds generated using “long crack” methods, such as those described above, have been challenged by small crack data. Long and small cracks have been traditionally defined with respect to the material microstructure, where a small crack is on the order of a grain or less. The developers of small crack data have repeatedly shown that cracks propagate at a stress level lower than the threshold defined using the constant  $R$  load reduction method. One method of generating small crack data is to use a compressive precracking scheme [21,22] to generate a fatigue crack from a notch that has little plastic history. The original specimen is then modified to only include the fatigue crack; the notched material is machined away, such that the new crack length is less than 1 mm [23]. This small crack can then be used to evaluate the material response with a “naturally initiated” fatigue crack. Furthermore, if the specimen is unmodified, a “history free” long fatigue crack can be used to investigate the effects of load history. Propagating this crack under constant amplitude load will generate steady state fatigue crack growth rate data [24,25].

In this paper the authors develop fatigue crack growth threshold data for 7075-T73 aluminum using the constant  $R$  and constant  $K_{\max}$  load reduction methods and a compressive precracking, constant amplitude loading scheme. Testing will be conducted at low and high stress ratio levels to investigate the implications of load history. A computational study will be performed using the principles of plasticity induced crack closure to attempt to explain any history effects observed. Finally, the authors will investigate the effects of small fatigue cracks on the fatigue crack growth threshold in this aluminum alloy.

## 2. Threshold testing procedures

The constant  $R$  load reduction method generates fatigue crack growth rates into the threshold region by reducing the applied load on the specimen in a controlled manner such that the load ratio,  $R$ , remains constant, e.g. the maximum and minimum load are continuously reduced throughout the test. The constant  $K_{\max}$  load reduction method also reduces both the maximum and minimum load to generate threshold data, however the value of  $K_{\max}$  is constant, i.e.  $R$  increases. The rate of load shedding for both methods is defined by the equation

$$C = \left( \frac{1}{K} \right) \left( \frac{dK}{da} \right) \quad (1)$$

where  $C$  is the normalized  $K$  gradient and is algebraically limited to a value greater than  $-80/m$  [9]. Fig. 1 graphically depicts the constant  $R$  test procedure as a blue short-dashed curve and the constant  $K_{\max}$  procedure as a black long-dashed curve. In this study, two specimen geometries were used to generate threshold data; the compact tension specimen,  $C(T)$ , and a middle through crack specimen,  $M(T)$ . For the case of a  $C(T)$  specimen, the stress intensity factor range is defined as

$$\Delta K = \frac{\Delta P}{B\sqrt{W(1-\alpha)^{3/2}}} (0.886 + 4.64\alpha - 13.32\alpha^2 + 14.72\alpha^3 - 5.6\alpha^4) \quad (2)$$

where  $\alpha = a/W$  for  $a/W \geq 0.2$  [26],  $\Delta P$  is the applied load range,  $W$  is the width of the specimen,  $B$  is the thickness of the specimen and  $a$  is the crack length. The stress intensity solution for an  $M(T)$  specimen is given as

$$\Delta K = \frac{\Delta P}{B} \sqrt{\frac{\pi\alpha}{2W} \sec \frac{\pi\alpha}{2}} \quad (3)$$

where  $\alpha = 2a/W$  for  $2a/W < 0.95$  [27],  $B$  is the specimen thickness and  $W$  is the width. For this study, the dimensions of the  $C(T)$  specimens were  $W = 76.2$  mm,  $B = 12.7$  mm, and an initial notch length of 19.1 mm. The  $M(T)$  dimensions were  $W = 76.2$  mm,  $B = 12.7$  mm and the initial notch length is 12.7 mm. ASTM standard E647 has detailed schematics of these specimens. The load reduction tests were precracked at a constant  $\Delta K$  that is equivalent to the first data point in the load reduction test. These loads were applied until the crack length was approximately  $a/W$  of 0.3.

A constant amplitude loading scheme was implemented to produce fatigue crack growth data with minimal load history effects. This was accomplished by

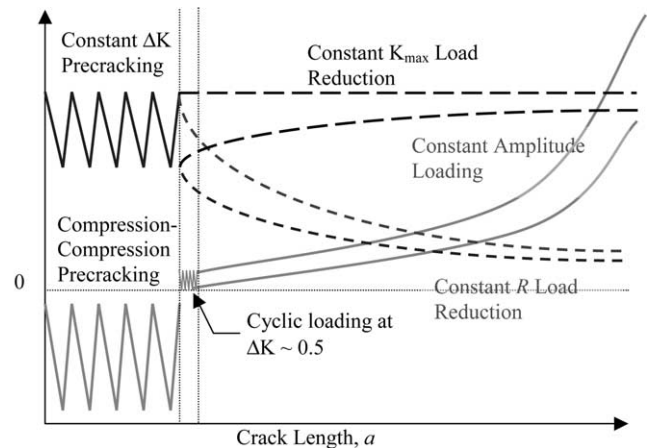


Fig. 1. Test methods for experimentally determining fatigue crack growth thresholds.

first producing a crack from a notch using a high compression scheme based on the closure-free test procedures proposed by Hubbard [28]. The precracking loads, both maximum and minimum loads in compression, were applied until the crack growth rate was less than  $10^{-10}$  m/cycle. Typically, this load produced a  $K_{\max}$  of  $-0.06$  MPa  $\text{m}^{1/2}$  and a  $K_{\min}$  of  $-19.9$  MPa  $\text{m}^{1/2}$ , computed using Eqs. (2) and (3), and required approximately 10,000 cycles. Then, the crack was propagated using a small tensile load, approximately  $K_{\max}$  of  $0.45$  MPa  $\text{m}^{1/2}$  and a  $K_{\min}$  of  $0.05$  MPa  $\text{m}^{1/2}$ , to grow out of the residual tensile stress field developed by the compressive loading. This crack propagation typically occurred rapidly, within the first 1000 cycles, and  $\Delta a$  never exceeded  $0.25$  mm before crack arrest occurred ( $da/dN < 10^{-12}$  m/cycle). Finally, constant amplitude loading was applied to generate fatigue crack growth rate data at a specific stress intensity range,  $\Delta K$ , and  $R$  value near threshold ( $da/dN \sim 10^{-10}$  m/cycle). Fig. 1 graphically depicts the constant amplitude load procedure as a red solid curve.

### 3. Crack closure

Many investigators have shown experimentally that the stress-intensity factor threshold under load-reduction schemes can be explained by crack-closure behavior, or a rise in crack opening level as the threshold is approached [29–31]. A number of suggestions have been advanced to explain the rise in the crack opening level. Among these are the mismatch of crack-surface features observed by Walker and Beevers [32]; the corrosion product formation on the crack surfaces, as observed by Paris et al. [33] and measured by Vasudevan and Suresh [34]; and plasticity-induced crack-closure as calculated by Newman [35]. The mismatch of crack-surface features and corrosion products on the crack surfaces can cause the surfaces to come into contact at a higher load than the load for a crack without mismatch or corrosion products. The mode of crack growth near the threshold is a combination of Mode I and II (tensile and shear). The mixed-mode crack growth, and permanent plastic deformations, causes an irregular crack-surface profile and mismatch, and, consequently, the possibility of premature crack-surface contact. The analytical treatment of crack closure due to crack-surface mismatch or corrosion products on the crack surface is beyond the scope of the present paper. Only the effects of residual-plastic deformations were considered in this paper.

The calculations performed herein were made with FASTRAN, a code capable of modeling plasticity-induced crack-closure for a through crack in a finite-width plate subjected to remote applied stress. The model is based on the Dugdale strip-yield model [36] but modified to leave plastically deformed material in

the wake of the crack. The details of the model are given elsewhere [37] and will not be presented here. One of the most important features of the model is the ability to model three-dimensional constraint effects. A constraint factor,  $\alpha$ , is used to elevate the flow stress ( $\sigma_o$ ) at the crack tip to account for the influence of stress state ( $\alpha\sigma_o$ ) on plastic-zone sizes and crack-surface displacements. The flow stress  $\sigma_o$  is taken as the average between the yield stress  $\sigma_{ys}$  and ultimate tensile strength  $\sigma_u$  of the material. For plane-stress conditions,  $\alpha$  is equal to unity (original Dugdale model); and for simulated plane-strain conditions,  $\alpha$  is equal to 3. Although the strip-yield model does not model the correct yield-zone shape for plane-strain conditions, the model with a high constraint factor is able to produce crack-surface displacements and crack-opening stresses quite similar to those calculated from three-dimensional, elastic-plastic, finite-element analyses of crack growth and closure for finite-thickness plates [38].

The opening stress can be used to develop an effective stress intensity factor,  $\Delta K_{\text{eff}}$  which has been used to generate “closure free” fatigue crack growth rate curves, i.e.  $da/dN$  vs.  $\Delta K_{\text{eff}}$ . This proves useful for evaluating the effects of plasticity induced closure on various experiments. The equations for computing the opening stress are a complex function of cyclic stress, load history, crack and specimen geometry, constraint and the element density used for calculating the plastic zone size. Fortunately, this series of equations can be simplified, assuming a positive stress ratio and  $\alpha = 2$ , such that the effective stress intensity factor range,  $\Delta K_{\text{eff}}$ , can be related to the stress intensity factor range,  $\Delta K$ , and the stress ratio,  $R$ , such that

$$\Delta K_{\text{eff}} = \Delta K(0.7 - 1.1R^2 + 0.4R^3)/(1 - R) \quad (4)$$

The assumption of a constraint value of 2 has been shown to be reasonable for 12.7 mm thick specimens manufactured from aluminum alloys [39]. Furthermore, solving Eq. (4) for  $\Delta K$  can be used to predict the fatigue crack growth behavior at a specific stress ratio. This prediction can then be used to estimate a starting stress level after compression precracking to generate threshold data.

### 4. Experimental data

C(T) specimens were tested utilizing a software-control system on a servo-hydraulic machine with a clip gage to measure compliance and determine crack length. The compliance crack length measurements were verified visually with a floating microscope. The M(T) specimens were tested using a function generator on a servo-hydraulic machine and the crack lengths were measured visually on both front and back surfaces using floating microscopes. All tests were conducted in lab air at a mean temperature of  $21^\circ\text{C}$  and a relative humidity of

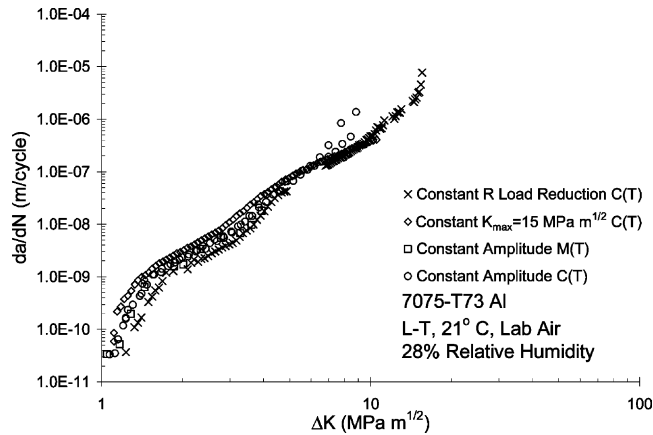


Fig. 2. Fatigue crack growth rate data at high  $R$  for 7075-T73 aluminum.

28%. The material was heat treated and annealed to the –T73 condition and all specimens were cut to produce data in the long-transverse grain orientation (L–). Each specimen was used for a single experiment and fatigued to failure, i.e. one curve was generated per specimen. All load reduction tests were conducted at a load shedding rate of  $-80/\text{m}$ .

#### 4.1. Constant $R$ load reduction

Constant  $R$  load reduction tests were performed at  $R = 0.1$  and  $R = 0.7$  using C(T) specimens. Specimens were precracked using a constant  $\Delta K$  consistent with the first data point in the load reduction scheme, and yielded an average threshold of  $2.30 \text{ MPa m}^{1/2}$  at  $R = 0.1$  and  $1.23 \text{ MPa m}^{1/2}$  at  $R = 0.7$ . A constant  $R$  load increasing test was conducted following the threshold test to generate the remaining fatigue crack growth rate curve. The  $R = 0.7$  and  $0.1$  data are presented in Figs. 2 and 3, respectively.

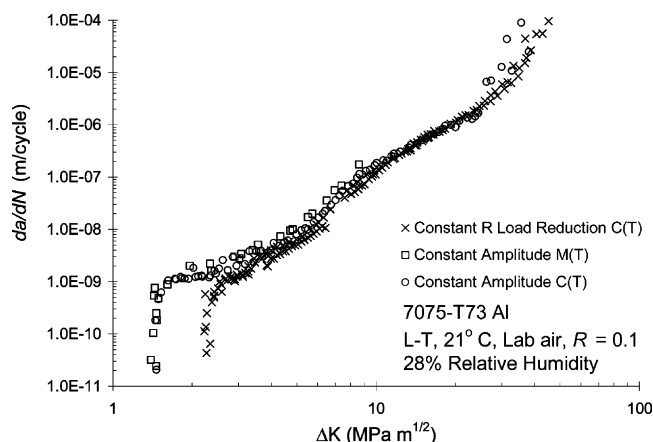


Fig. 3. Fatigue crack growth rate data at  $R = 0.1$  for 7075-T73 aluminum.

#### 4.2. Constant $K_{\max}$ load reduction

Constant  $K_{\max}$  tests were conducted using both C(T) and M(T) specimens in an attempt to determine the threshold values for this material. Constant  $K_{\max}$  load reduction tests were conducted at  $K_{\max}$  levels of 15, 2.20 and  $1.65 \text{ MPa m}^{1/2}$ . A C(T) specimen was precracked at a constant  $K_{\max}$  of  $15 \text{ MPa m}^{1/2}$  at  $R = 0.1$  until  $a/W$  was approximately 0.3. The constant  $K_{\max}$  load reduction test was then conducted yielding a threshold of  $1.11 \text{ MPa m}^{1/2}$  at  $R = 0.95$ . The M(T) specimens were precracked in compression at a  $K_{\max}$  of  $-0.06 \text{ MPa m}^{1/2}$  and a  $K_{\min}$  of  $-19.9 \text{ MPa m}^{1/2}$  with a notch width of 12.7 mm. The crack propagated approximately 1.27 mm before the crack growth rate fell below  $10^{-10} \text{ m/cycle}$ . At which time, the crack was propagated using a small tensile load, approximately  $K_{\max}$  of  $0.45 \text{ MPa m}^{1/2}$  and a  $K_{\min}$  of  $0.05 \text{ MPa m}^{1/2}$ , to grow out of the residual tensile stress field developed by the compressive loading. Specimens were then tested at a constant  $K_{\max}$  of  $2.20 \text{ MPa m}^{1/2}$  to produce a threshold of  $0.95 \text{ MPa m}^{1/2}$  at an  $R$  of 0.57 and two specimens were tested at a constant  $K_{\max}$  of  $1.65 \text{ MPa m}^{1/2}$  to achieve a threshold of  $1.86 \text{ MPa m}^{1/2}$  at  $R = -0.13$  and  $1.65 \text{ MPa m}^{1/2}$  at an  $R$  of 0.00. The data produced from the constant  $K_{\max}$  load reduction tests is shown in Figs. 2 and 4. Once the threshold rate was achieved ( $10^{-10} \text{ m/cycle}$ ), constant amplitude loading was applied at the same  $\Delta K$  and  $R$  value of the just established threshold to generate a constant  $R$  fatigue crack growth curve. These results are also plotted in Fig. 4.

#### 4.3. Constant amplitude

Using the threshold value generated with the constant  $K_{\max} = 15 \text{ MPa}$  test, assuming the constant  $K_{\max}$  threshold to represent a  $\Delta K_{\text{eff}}$  threshold, and solving Eq. (4) for  $\Delta K$ , the threshold for  $R = 0.1$  could be estimated to be  $1.45 \text{ MPa m}^{1/2}$  and the threshold at  $R = 0.7$  could be

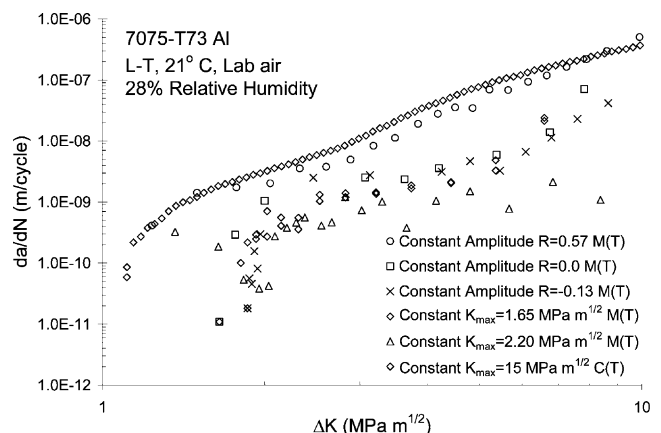


Fig. 4. Fatigue crack growth rate data constant  $K_{\max}$  followed by constant amplitude loading for 7075-T73 aluminum.

estimated to be  $1.04 \text{ MPa m}^{1/2}$ . Therefore,  $M(T)$  and  $C(T)$  specimens were precracked using the same compression scheme described above, then a constant amplitude load was applied that would develop a  $\Delta K$  value near threshold for  $R = 0.1$  and  $0.7$ . These values were  $1.45 \text{ MPa m}^{1/2}$  for the  $R = 0.1$  case and  $1.04 \text{ MPa m}^{1/2}$  for  $R = 0.7$ . The fatigue crack growth curves generated using this method are shown in Fig. 2 for  $R = 0.7$  and Fig. 3 for  $R = 0.1$ .

## 5. Observations

It is apparent that the constant  $R$  load reduction procedure develops a threshold that is nearly twice that of a constant amplitude test using a  $C(T)$  specimen in 7075-T73 aluminum (Fig. 3) at  $R = 0.1$ . The authors postulate that this is an artifact of the load history. Assuming that large plastic strains exist in the crack wake imparted from the higher initial loads, as the load reduction test persists, remote crack closure will occur prematurely unloading the crack tip, resulting in an artificially high threshold. A simulation of the constant  $R$  load reduction test procedure, using FASTRAN, for a typical aluminum alloy ( $\alpha = 2$ ) is shown in Fig. 5. Plotted are the local crack opening displacements (CODs) along the crack surfaces for a simulated test at  $R = 0.1$ . The notch, fatigue precracking (constant-amplitude loading at  $(S_{\max})_{CA} = 120 \text{ MPa}$ ), and load-reduction regions are as indicated along the  $x$ -axis. The solid and dashed curves show the results at maximum and minimum applied stress, respectively. These results show that the crack surfaces were not in contact at the maximum applied stress ( $6.8 \text{ MPa}$ ). But at the minimum applied stress, the crack surfaces near the start of the load-reduction procedure and over a very small region at the crack tip ( $a = 59 \text{ mm}$ ) were closed. The remote closure reduces the effective stress-intensity factor range at the crack tip,

which causes the threshold to develop at a higher stress-intensity factor range [40].

It is also apparent that there is little difference between the threshold value determined at  $R = 0.7$  using the different approaches (Fig. 2). It has been proposed that  $R = 0.7$  data are near closure free since the crack is kept open at the higher  $R$  values. Therefore, It would stand to reason that if there is no change in threshold data based on different specimen geometries, that the aberrations witnessed in the  $R = 0.1$  data could be attributable to load history effects. Utilizing the constant amplitude loading scheme,  $M(T)$  and  $C(T)$  specimens were tested at the  $R = 0.1$  condition to identify any geometric effects. The variation in the fatigue crack growth rate curve, even at threshold, is insignificant between the different geometries, as can be seen in Fig. 3. Hence, the different crack growth behavior illustrated in Fig. 3 must be attributable to load history effects inducing closure, as the  $K_{\max}$  levels were assumed low enough to avoid inducing creep.

Utilizing the effective stress intensity factor,  $\Delta K_{\text{eff}}$ , as defined in Eq. (4), the fatigue crack growth rate data can be used to collapse to generate a single curve [37]. The effective stress intensity factor curve can then be used to predict where fatigue crack growth rate curves will exist for specific  $R$  values. Using this approach, the constant amplitude  $R = 0.7$  data were assumed to be “closure free” for generating a  $da/dN$  vs.  $\Delta K_{\text{eff}}$  curve and predicting where the closure corrected  $R = 0.1$  curve would lie. The results of this exercise are shown in Fig. 6. It is interesting to note that the spread of fatigue crack growth thresholds that is traditionally cited in the literature is reflective of the constant  $R$  load reduction test method. When comparing the constant amplitude data, which is steady-state, this trend does not exist.

It has been argued that small cracks behave differently than long cracks in aluminum. Based on experimental data, small cracks propagate at stress intensity factors much lower than corresponding long cracks. Small crack data for 7075-T6 in the L-T grain orientation were found

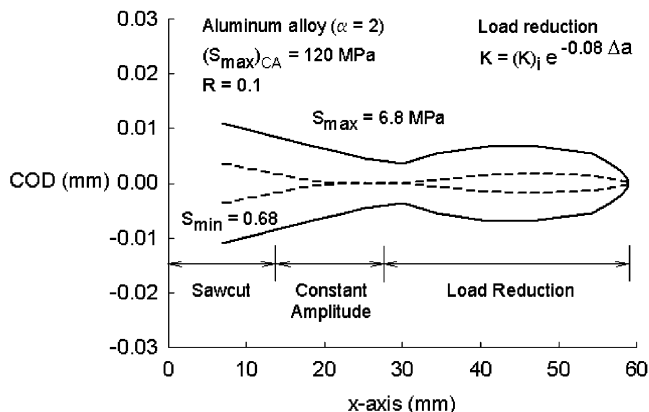


Fig. 5. Crack-surface displacements after load reduction under  $\alpha = 2$  constraint conditions.

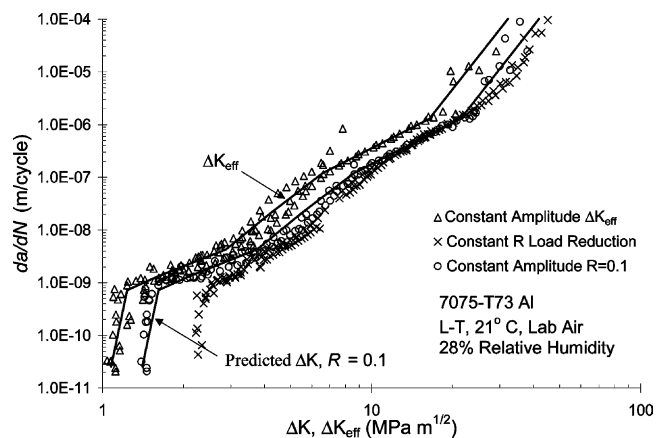


Fig. 6. Effective stress intensity factor data for 7075-T73 aluminum.

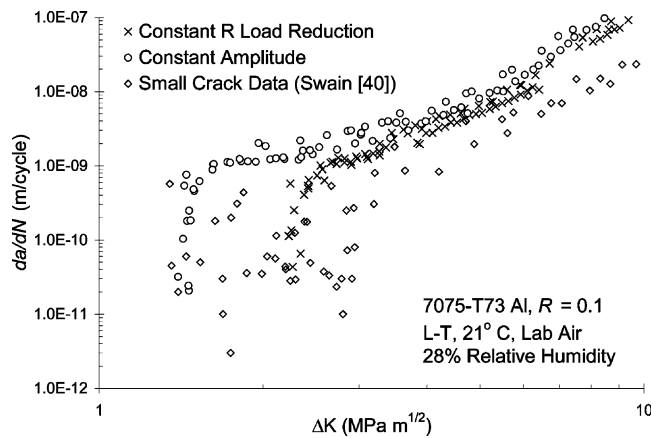


Fig. 7. Small crack data at threshold for 7075-T73 aluminum.

in the literature for  $R = -1$  [41]. Using Eq. (4), these data were translated to  $R = 0.1$  and plotted against the 7075-T73 data generated herein. The constant amplitude long crack data encompass the small crack data, implying that the short and long crack thresholds are merely an artifact of the constant  $R$  load reduction test procedure. These data are plotted in Fig. 7 along with the constant  $R$  load reduction data for reference.

## 6. Conclusions

Investigating the impact a test procedure has on the data being generated is important in order to understand material response. If the test procedure alters the data by introducing effects, such as remote closure, the test is not adequately describing the material behavior. In the case of fatigue crack growth thresholds, where the threshold is traditionally considered to be a safe value where no crack growth occurs, accurate representation of the material behavior and subsequent component fatigue life is crucial. Using the constant  $R$  load reduction test will generate artificially high threshold values when compared to steady-state data. This level of unconservatism will vary significantly from material to material. Since this variability is currently unknown, computational tools can be used to predict lower stress ratio fatigue crack growth rate behavior, such as  $\Delta K_{\text{eff}}$ , until experimental data can be generated. Furthermore, it is clear that in 7075-T73 aluminum there is no “short/long crack anomaly”. The load history effects introduced into the long crack data has generated a database of artificially high thresholds that do not accurately represent the material response of cracks growing under increasing  $K$ .

## References

[1] Paris PC, Erdogan F. A critical analysis of crack propagation laws. Transactions of the ASME, Journal of Basic Engineering, Series D 1963;85(3).

[2] Barsom JM. Fatigue-crack propagation in steels of various yield strengths. Transactions of the ASME, Journal of Engineering for Industry, Series B 1971;93(4).

[3] Frost NE. The growth of fatigue cracks. In: Proceedings of the First International Conference on Fracture; Sendai, Japan; 1966. p. 1433.

[4] Bucci RJ. Development of a proposed ASTM standard test method for near-threshold fatigue crack growth rate measurement. In: Fatigue crack growth measurement and data analysis, ASTM STP 738. ASTM; 1981. p. 5–28.

[5] Pearson S. Initiation of fatigue cracks in commercial aluminum alloys and the subsequent propagation of very short cracks. Engineering Fracture Mechanics 1975;7(2):235–47.

[6] Taylor D, Knott JF. Fatigue crack propagation behavior of short cracks—the effects of microstructure. Fatigue of Engineering Materials and Structures 1981;4(2):147–55.

[7] Taylor D, Knott JF. Growth of fatigue cracks from casting defects in nickel aluminum bronze. In: Proceedings of the Metal Society Conference on Defects and Crack Initiation in Environment Sensitive Fracture; University of Newcastle-on-Tyne; 1981.

[8] Lankford J. The growth of small fatigue cracks in 7075-T6 aluminum. Fatigue of Engineering Materials and Structures 1985;5(3):233–48.

[9] Hudak SJ Jr, Saxena SJ, Bucci A, Malcolm RC. Development of standard methods of testing and analyzing fatigue crack growth rate data—final report. AFML TR 78-40, Air Force Materials Laboratory, Wright Patterson Air Force Base, OH; 1978.

[10] Minakawa K, Newman Jr JC, McEvily AJ. A critical study of the closure effect on near-threshold fatigue crack growth. Fatigue and Fracture of Engineering Materials and Structures 1983;6:359.

[11] Wu XJ, Wallace W, Koul AK. A new approach to fatigue threshold. Fatigue and Fracture of Engineering Materials and Structures 1995;18(7-8):833–45.

[12] Chen DL, Weiss B, Stickler R. Effect of stress ratio and loading condition on the fatigue threshold. International Journal of Fatigue 1992;14:325–9.

[13] Elber W. Crack-closure and crack-growth measurements in surface-flawed titanium alloy Ti-6Al-4V. NASA TN D-8010; 1975.

[14] Smith SW, Piascik RS. An indirect technique for determining closure-free fatigue crack growth behavior. In: Fatigue crack growth thresholds, endurance limits, and design, ASTM STP 1372. ASTM; 2000. p. 109–22.

[15] Herman WA, Hertzberg RW, Jaccard R. A simplified laboratory approach for the prediction of short crack behavior in engineering structures. Fatigue and Fracture of Engineering Materials and Structures 1988;11(4):303–20.

[16] Hertzberg R, Herman WA, Clark T, Jaccard R. Simulation of short crack and other low closure loading conditions utilizing  $K_{\text{max}}$   $\Delta K$ -decreasing fatigue crack growth procedures. In: Small crack test methods, ASTM STP 1149. ASTM; 1991. p. 197–220.

[17] Bush RW, Donald JK, Bucci RJ. Pitfalls to avoid in threshold testing and its interpretation. In: Fatigue crack growth thresholds, endurance limits, and design, ASTM STP 1372. ASTM; 2000. p. 269–84.

[18] Newman JA, Riddell WT, Piascik RS. Effects of  $K_{\text{max}}$  on fatigue crack growth threshold in aluminum alloys. In: Fatigue crack growth thresholds, endurance limits, and design, ASTM STP 1372. ASTM; 2000. p. 63–77.

[19] Hertzberg RW, Herman WA, Ritchie RO. Use of a constant  $K_{\text{max}}$  test procedure to predict small crack growth behavior in -T8E41 aluminum-lithium alloy. Scripta Metallurgica 2090;21(1987):1541–6.

[20] Marci G. Fatigue crack propagation threshold: what is it and how is it measured? Journal of Testing and Evaluation 1998;26(3):220–33.

[21] Topper TH, Au P. Cyclic strain approach to fatigue in metals.

- In: AGARD lecture series 118, Fatigue test methodology, 1981 Oct 19–20; Technical University of Denmark, Denmark.
- [22] Conle A, Topper TH. Evaluation of small cycle omission criteria for shortening of fatigue service histories. *International Journal of Fatigue* 1979; Jan.
- [23] Christman T, Suresh S. Crack initiation under far-field cyclic compression and the study of short fatigue cracks. *Engineering Fracture Mechanics* 1986;23(6):953–64.
- [24] Suresh S. Crack initiation in cyclic compression and its applications. *Engineering Fracture Mechanics* 1985;21:453.
- [25] Pippan R, Plochl L, Klanner F, Stuwe HP. The use of fatigue specimens precracked in compression for measuring threshold value and crack growth. *Journal of Testing and Evaluation* 1994;22(2):98–103.
- [26] Newman JC Jr. Stress analysis of the compact specimen including the effects of pin loading. In: *Fracture analysis*, ASTM STP 560. ASTM; 1974. p. 105–21.
- [27] Feddersen CE. Discussion of plane-strain crack toughness testing of metallic materials. In: *Current status of plane strain crack toughness testing of high-strength metallic materials*, ASTM STP 410. ASTM; 1967. p. 77–9.
- [28] Hubbard RP. Crack growth under cyclic compression. *Journal of Basic Engineering, Transactions of ASME* 1969;91.
- [29] Ohta A, Kosuge M, Sasake E. Fatigue crack closure over the range of stress ratios from  $-1$  to  $0.8$  down to stress intensity factor threshold level in HT80 steel and SUS 304 stainless steel. *International Journal of Fracture* 1978;14(3):251–64.
- [30] Minakawa K, McEvily AJ. On crack closure in the near-threshold region. *Scripta Metallurgica* 1981;15:633–6.
- [31] Donald JK, Paris PC. An evaluation of  $\Delta K_{\text{eff}}$  estimation procedures on 6061-T6 and 2024-T3 aluminum alloys. In: *Proceedings of fatigue damage of structural materials II*, 1998 Sep 7–11; Cape Cod, MA.
- [32] Walker N, Beevers CJ. A fatigue crack closure mechanism in titanium. *Fatigue of Engineering Materials and Structures* 1979;1(1):135–48.
- [33] Paris PC, Bucci RJ, Wessel ET, Clark WG, Mager TR. Extensive study of low fatigue crack growth rates in A533 and A508 steels, ASTM STP-513. ASTM; 1972. p. 141–76.
- [34] Vasudevan AK, Suresh S. Influence of corrosion deposits on near-threshold fatigue crack growth behavior in 2XXX and 7XXX series aluminum alloys. *Metallurgical Transactions A* 1982;13A:2271–80.
- [35] Newman JC Jr. A nonlinear fracture mechanics approach to the growth of small cracks. In: *Behavior of short cracks in airframe materials*, AGARD CP-328; 1983. p. 6.1–6.26.
- [36] Dugdale DS. Yielding of steel sheets containing slits. *Journal of the Mechanics and Physics of Solids* 1960;8:100–4.
- [37] Newman JC, Jr. A crack-closure model for predicting fatigue crack growth under aircraft spectrum loading. In: *Methods and models for predicting fatigue crack growth under random loading*, ASTM STP 748. ASTM; 1981. p. 53–84.
- [38] Blom A, Wang G, Chermahini RG. Comparison of crack closure results obtained by 3D elastic-plastic FEM and modified Dugdale model. In: *Localized damage: computer-aided assessment and control*. Berlin: Computational Mechanics Publications, Springer-Verlag; 1990. p. 57–68.
- [39] Newman JC Jr. An evaluation of the plasticity-induced crack-closure concept and measurement methods. NASA TM 208430; 1998.
- [40] Newman JC Jr. Analysis of fatigue crack growth and closure near threshold conditions. In: *Fatigue growth thresholds*, ASTM STP-1372. ASTM; 2000. p. 227–51.
- [41] Swain MH, Newman JC Jr., Phillips EP, Everett RA Jr. Fatigue crack initiation and small crack growth in several airframe alloys, NASA TM-102598; Jan 1990.